INTERNATIONAL JOURNAL FOR NUMERICAL METHODS IN ENGINEERING
Int. J. Numer. Meth. Engng 2003; **58**:1985–2011 (DOI: 10.1002/nme.843)

A polynomial collocation method for the numerical solution of weakly singular and singular integral equations on non-smooth boundaries

G. Monegato*,† and L. Scuderi

Dipartimento di Matematica, Politecnico di Torino, Corso Duca degli Abruzzi 24, 10129 Turin, Italy

SUMMARY

The aim of this paper is to show the efficiency of the use of smoothing changes of variable in the numerical treatment of 1D and 2D weakly singular and singular integral equations. The introduction of a smoothing transformation, besides smoothing the solution, allows also the use of a very simple and efficient collocation method based on Chebyshev polynomials of the first kind and their zeros.

Further, we propose proper smoothing changes of variable also for the numerical approximation of those collocation matrix elements, which are given by weakly singular, singular or nearly singular integrals.

Several numerical tests are given to point out the efficiency of the numerical approach we propose.

KEY WORDS: boundary integral equations; polynomial collocation methods; numerical integration

1. INTRODUCTION

In this paper we consider the Laplace equation in 2D and in 3D, defined on domains Ω with piecewise smooth boundaries Γ and associated with boundary conditions that can be of Dirichlet type or, more generally, of mixed type of the form

$$\begin{aligned} \Delta u &= 0 \quad \text{on } \Omega \\ u &= f_1 \quad \text{on } \Gamma_D \\ \frac{\partial u}{\partial \mathbf{n}} &= f_2 \quad \text{on } \Gamma_N \end{aligned} \tag{1}$$

where $\Gamma = \Gamma_D \cup \Gamma_N$.

*Correspondence to: G. Monegato, Dipartimento di Matematica, Politecnico di Torino, Corso Duca degli Abruzzi 24, 10129 Turin, Italy.
†E-mail: monegato@polito.it

Contract/grant sponsor: Ministero dell'Università e della Ricerca Scientifica e Tecnologica
Contract/grant sponsor: Consiglio Nazionale delle Ricerche; contract/grant number: 98.00648.CT11

Received 28 March 2002
Revised 13 January 2003
Accepted 20 January 2003

In particular, we use the single layer representation of the potential to reformulate the problem as a classical boundary integral equation. For instance, in 2D we write

$$u(P) = -\frac{1}{\pi}\int_{\Gamma} \log|P-Q|\bar{z}(Q)\,\mathrm{d}\Gamma_Q \quad P \in \Omega \tag{2}$$

where $|P-Q|$ is the Euclidian distance between P and Q, $\mathrm{d}\Gamma_Q$ is the arc-length element and $\bar{z}$ is an unknown function called 'single layer density'.

In the case of (1) we obtain the following final system for the unknown $\bar{z}$:

$$\begin{aligned} -\frac{1}{\pi}\int_{\Gamma} \log|P-Q|\bar{z}(Q)\,\mathrm{d}S_Q &= f_1(P) \quad P \in \Gamma_D \\ \bar{z}(P) - \frac{1}{\pi}\int_{\Gamma} \frac{\partial \log|P-Q|}{\partial \mathbf{n}_P}\bar{z}(Q)\,\mathrm{d}S_Q &= f_2(P) \quad P \in \Gamma_N \end{aligned} \tag{3}$$

Once we know $\bar{z}$ on Γ the solution $u(P)$ of problem (1) on Ω can be determined using (2).

While the case of smooth boundaries has been discussed extensively (see Reference [1]), the case of boundaries $\Gamma = \bigcup_{i=1}^{l} \Gamma_i$ which are only piecewise smooth have been considered properly more recently. In the latter situation several collocation and Galerkin methods have been examined (see Reference [1] and the references cited there).

A recent novel approach suggests (see, for instance, References [2–12]) to reformulate the integral equations in terms of a new unknown which is as smooth as one likes in the domain of integration. This is accomplished by combining a parametrization of the boundary Γ with a smoothing change of variable. Using this smoothing strategy, in References [5–7, 9], we have applied a collocation method associated with a global polynomial approximation. Stability and convergence estimates have then been obtained. From a theoretical point of view, this strategy allows to achieve arbitrarily high orders of convergence.

In the papers [5–7, 9] the whole curve Γ is mapped onto a reference (bounded) interval I, and the unknown function is approximated over I by a global polynomial. In this paper we examine a variant of this approach, which in our opinion should be more efficient and flexible. In particular, after having introduced a smoothing function on each smooth piece Γ_i of the curve Γ, we propose to approximate the unknown by a different polynomial on each Γ_i. Therefore our new approximant is not any longer formed, as in References [5–7, 9], by a unique polynomial on the whole boundary Γ, but it is given by the composition of several polynomials: one for each Γ_i, $i = 1, \ldots, l$. Since our new unknown will have the same (desired) smoothness degree on each Γ_i, all our polynomials will have the same degree. Our method can thus be considered a p-method, where each element coincides with an arc Γ_i and all approximants have the same polynomial degree.

While this new method appears simple to apply and quite effective for 2D problems, at present its development does not seem to be competitive with other numerical techniques, such as $h-$, $h-p$ methods, in the case of 3D problems. Several numerical examples will be presented in the next sections, for 2D and 3D problems.

We will also present a simple technique for the evaluation of the integrals required by our collocation method, when the collocation point is inside or very close to the domain of integration.

In Sections 2 and 3 (and their subsections) we will describe the smoothing approach and the numerical method we propose to solve a Dirichlet and a Neumann problem, respectively. In Section 4 we will present various numerical tests which show the efficiency of our numerical approach. Finally, in Section 5 we will apply an analogous smoothing strategy to a simple 3D Dirichlet problem.

2. THE DIRICHLET PROBLEM IN 2D

We first consider the Dirichlet problem for the Laplace equation

$$\begin{aligned} \Delta u &= 0 \quad \text{on } \Omega \\ u &= \bar{f} \quad \text{on } \Gamma = \bigcup_{i=1}^{l} \Gamma_i \end{aligned} \tag{4}$$

in a simply connected region Ω with piecewise smooth boundary Γ. Using the single layer representation (2) of u we derive the following Boundary Integral Equation (BIE)

$$-\frac{1}{\pi}\int_{\Gamma} \log|P-Q|\bar{z}(Q)\,\mathrm{d}S_Q = \bar{f}(P) \quad P \in \Gamma$$

or, equivalently,

$$-\frac{1}{\pi}\sum_{i=1}^{l}\int_{\Gamma_i} \log|P-Q|\bar{z}_i(Q)\,\mathrm{d}S_Q = \bar{f}(P) \tag{5}$$

where the unknowns $\bar{z}_i := \bar{z}|\Gamma_i$ are sought on Γ_i, $i = 1, \ldots, l$. To transform the above curvilinear 2D integrals into 1D integrals on the same reference interval, we introduce in (5) a parametrization $\bar{\alpha}_i$ defined on $[0,1]$ for each arc Γ_i,

$$\bar{\alpha}_i : s \in [0,1] \to \bar{\alpha}_i(s) := (\bar{\alpha}_{1,i}(s), \bar{\alpha}_{2,i}(s)) \in \Gamma_i \quad i = 1, \ldots, l$$

and we get

$$-\frac{1}{\pi}\sum_{i=1}^{l}\int_{0}^{1} \log|\bar{\alpha}_j(s) - \bar{\alpha}_i(\sigma)|\,\bar{z}_i(\bar{\alpha}_i(\sigma))\,|\bar{\alpha}_i'(\sigma)|\,\mathrm{d}\sigma = \bar{f}(\bar{\alpha}_j(s)) \quad j = 1, \ldots, l \tag{6}$$

From now on, we will denote by P_i the interface points of our boundary Γ and by β_i, with $0 < \beta_i < 2\pi$, the interior angle of Γ at P_i. Then, taking into account the behaviour of the function $\bar{z}$ near the corners P_i, which is given by

$$\bar{z}(P) = c(\theta) r^{s_i} + \text{smoother terms}, \quad s_i = \min\left\{\frac{\pi}{\beta_i}, \frac{\pi}{2\pi - \beta_i}\right\} - 1, \quad P \in \Gamma$$

being (r, θ) the polar co-ordinates centred at P_i (see, for instance, References [6, 10]), we suggest to introduce a smoothing change of variable. This improves the behaviour of the unknown

$\bar{z}$ near P_i, by incorporating the Jacobian of the transformation. As smoothing transformation we propose the following polynomial:

$$\gamma(t)=\frac{\int_0^t x^{q-1}(1-x)^{q-1}\,\mathrm{d}x}{\int_0^1 x^{q-1}(1-x)^{q-1}\,\mathrm{d}x} \quad q>1 \tag{7}$$

which is a nondecreasing function, mapping $(0,1)$ onto $(0,1)$ and satisfying the following endpoint conditions:

$$\gamma(0)=0, \quad \gamma(1)=1$$
$$\gamma^{(k)}(0)=\gamma^{(k)}(1)=0, \quad k=1,\ldots,q-1$$

This transformation, which represents a distribution much used in statistical applications, was already employed for dealing with endpoint singularities in References [5, 6, 9, 10, 13, 14]

The smoothing parameter q allows to control the degree of smoothness of the unknown function: the more q is large, the more the unknown is smooth. In practice, it is sufficient to take $q=2$ or 3 to derive a good accuracy already by solving low order linear systems. Therefore, for completeness we give the following explicit expressions:

$$\gamma(t)=\begin{cases}-t^2(2t-3) & \text{if } q=2\\ t^3(6t^2-15t+10) & \text{if } q=3\end{cases}$$

Introducing $\gamma(t)$ into (6) and setting $\tilde{\alpha}_j(t):=\bar{\alpha}_j(\gamma(t))$ we then have

$$-\frac{1}{\pi}\sum_{i=1}^{l}\int_0^1 \log|\tilde{\alpha}_j(t)-\tilde{\alpha}_i(\tau)|\bar{z}_i(\tilde{\alpha}_i(\tau))|\tilde{\alpha}_i'(\tau)|\,\mathrm{d}\tau=\bar{f}(\tilde{\alpha}_j(t)) \quad j=1,\ldots,l \tag{8}$$

The last crucial step before solving numerically the above integral equations is to map the interval of integration $[0,1]$ onto $[-1,1]$ and then to introduce the Chebyshev weight

$$w(x):=\frac{1}{\sqrt{1-x^2}}$$

This step is essential both from the theoretical and numerical points of view, because it is fundamental to deal with the integral

$$-\frac{1}{\pi}\int_{-1}^{1}\log|x-y|\frac{v(y)}{\sqrt{1-y^2}}\,\mathrm{d}y$$

either to derive a good numerical approximation of the integrals in (8), or to study theoretically the BIE and its numerical resolution. Its well-known special property, which plays a fundamental role, is

$$-\frac{1}{\pi}\int_{-1}^{1}\log|x-y|\frac{T_m(y)}{\sqrt{1-y^2}}\,\mathrm{d}y=\begin{cases}\ln 2\,T_0(x) & \text{if } m=0\\ \dfrac{1}{m}\,T_m(x) & \text{if } m\geqslant 1\end{cases} \tag{9}$$

Under the above considerations we rewrite the final form of our BIE as follows:

$$-\frac{1}{\pi}\sum_{i=1}^{l}\int_{-1}^{1}\log|\alpha_j(r)-\alpha_i(\rho)|\,\frac{z_i(\rho)}{\sqrt{1-\rho^2}}\,\mathrm{d}\rho=f_j(r)\quad j=1,\ldots,l \tag{10}$$

where we have set

$$\begin{aligned}&\alpha_i(\rho):=\tilde{\alpha}_i((\rho+1)/2)\\&z_i(\rho):=\bar{z}_i(\alpha_i(\rho))|\alpha_i'(\rho)|\sqrt{1-\rho^2}\quad f_j(r):=\bar{f}(\alpha_j(r))\end{aligned} \tag{11}$$

Note that in (11) the presence of the weight function does not spoil the degree of smoothness of the solutions z_i because in the Jacobian $|\alpha_i'|$ the factor γ' precisely absorbs the irregularities at the endpoints of the domain of integration; actually, it improves the smoothness of z_i at ± 1.

2.1. A Chebyshev collocation method

To solve numerically (10) we propose a collocation method, which uses Chebyshev orthogonal expansions as approximant of the unknown function z_i on each arc Γ_i, and the zeros of Chebyshev polynomials as collocation nodes. Therefore, using the following polynomial approximation

$$z_i(\rho)\sim z_{i,n}(\rho)=\sum_{h=1}^{n}a_{(i-1)n+h}\,T_{h-1}(\rho)\quad i=1,\ldots,l \tag{12}$$

where T_{h-1} is the classical first kind orthogonal Chebyshev polynomial of degree $h-1$, and the zeros of T_n

$$x_{n,k}=\cos\left(\frac{2(n-k)+1}{2n}\,\pi\right)\quad k=1,\ldots,n \tag{13}$$

as collocation nodes, the final collocation linear system of $n\times l$ equations is

$$-\frac{1}{\pi}\sum_{i=1}^{l}\sum_{h=1}^{n}a_{(i-1)n+h}\int_{-1}^{1}\log|\alpha_j(x_{n,k})-\alpha_i(\rho)|\,\frac{T_{h-1}(\rho)}{\sqrt{1-\rho^2}}\,\mathrm{d}\rho=f_j(x_{n,k})\quad k=1,\ldots,n,\ j=1,\ldots,l \tag{14}$$

To evaluate the matrix elements in (14) we have to compute (numerically) the integral

$$\begin{aligned}&I^S:=-\frac{1}{\pi}\int_{-1}^{1}\log|\alpha_j(r)-\alpha_i(\rho)|\,\frac{T_{h-1}(\rho)}{\sqrt{1-\rho^2}}\,\mathrm{d}\rho\\&r:=x_{n,k}\quad k,h=1,\ldots,n\ j\quad i=1,\ldots,l\end{aligned} \tag{15}$$

To this aim we suggest different procedures of integration according to the values of i and j, to the position of the collocation node r, to the smoothing parameter q of γ in (7) and to the parametrization $\tilde{\alpha}_i$ of the arc Γ_i of Γ. Therefore, we first distinguish the following

three cases:

$$\begin{aligned} &\text{(i)}\ j = i \\ &\text{(ii)}\ j = i-1, i+1 \\ &\text{(iii)}\ j \neq i, i-1, i+1 \end{aligned} \tag{16}$$

In the first case the collocation point belongs to the integration domain Γ_i, in the second one it lies on the arc Γ_j adjacent to that of integration Γ_i and in the third case we assume that the collocation point is far from Γ_i. Notice that in the latter situation we do not consider the case of two non-consecutive elements which are however very close to each other. This certainly is a situation which gives rise to severe difficulties in the evaluation of the corresponding integrals, since it is associated with a kernel having complex conjugate poles very close to the element of integration. The description of how to overcome this difficulty is quite involving and we have preferred to omit it.

Note that in case (i) the log-kernel admits a real singularity at $\rho = r$. Nevertheless, if $\bar{\alpha}_i$ is linear and $q = 1$, the integral can be evaluated analytically by virtue of (9); in the other cases we need to proceed numerically. However, before applying any quadrature formula it is convenient to rewrite the integral (15) in the following form:

$$I^S = -\frac{1}{\pi}\int_{-1}^{1} \log\frac{|\alpha_i(r)-\alpha_i(\rho)|}{|r-\rho|}\frac{T_{h-1}(\rho)}{\sqrt{1-\rho^2}}\,\mathrm{d}\rho - \frac{1}{\pi}\int_{-1}^{1}\log|r-\rho|\frac{T_{h-1}(\rho)}{\sqrt{1-\rho^2}}\,\mathrm{d}\rho =: A_1 + A_2 \tag{17}$$

where A_2 is known analytically and the log-kernel in A_1 is smooth, being r fixed and inside the interval $(-1,1)$ and α_i smooth.

In our practical examples, for the computation of A_1 we have used a classical Gauss–Chebyshev (G–C) quadrature formula with $m = 2n$ quadrature nodes, where n is the number of the collocation nodes for each arc. Moreover, we have adopted some numerical tricks when r and ρ, or $\gamma((r+1)/2)$ and $\gamma((\rho+1)/2)$, have a relative distance of the order of the machine precision *eps* or less. Indeed, in these cases, the log-argument suffers from severe loss of accuracy, because of numerical cancellation. To avoid this latter we then have used the following expression:

$$\begin{aligned} \log\frac{|\alpha_i(r)-\alpha_i(\rho)|}{|r-\rho|} &= \log\left(\frac{|\bar{\alpha}_i(\gamma((r+1)/2)) - \bar{\alpha}_i(\gamma((\rho+1)/2))|}{|\gamma((r+1)/2)-\gamma((\rho+1)/2)|}\,\frac{|\gamma((r+1)/2)-\gamma((\rho+1)/2)|}{|r-\rho|}\right) \\ &= \log\frac{|\bar{\alpha}_i(\gamma((r+1)/2)) - \bar{\alpha}_i(\gamma((\rho+1)/2))|}{|\gamma((r+1)/2)-\gamma((\rho+1)/2)|} + \log|a(\rho)| \end{aligned} \tag{18}$$

with

$$a(\rho) = \gamma'\left(\frac{r+1}{2}\right)\frac{1}{2} + \gamma''\left(\frac{r+1}{2}\right)\frac{(\rho-r)}{2^2\,2!} + \cdots + \gamma^{(2q-1)}\left(\frac{r+1}{2}\right)\frac{(\rho-r)^{2q-2}}{2^{2q-1}(2q-1)!}$$

and the approximation

$$\log\frac{|\alpha_i(r)-\alpha_i(\rho)|}{|r-\rho|} \approx \log|\alpha_i'(r)| \tag{19}$$

when $|r-\rho| \leqslant eps$, or

$$\log \frac{|\alpha_i(r)-\alpha_i(\rho)|}{|r-\rho|} \approx \log \left| \bar{\alpha}_i' \left(\gamma \left(\frac{r+1}{2} \right) \right) \right| + \log |a(\rho)| \tag{20}$$

when $|\gamma((r+1)/2) - \gamma((\rho+1)/2)| \leqslant eps$.

Note that because of the flatness of γ in the neighbourhood of the endpoints ± 1 when q is large, it may happen that $\gamma((r+1)/2) \approx \gamma((\rho+1)/2)$ even if r and ρ are far away. Note also that if Γ is a polygon, and hence $\bar{\alpha}_i$ is linear, the terms to the right and left hand side of (20) are equal.

In cases (ii) and (iii) we have applied a G–C formula directly to the integral (15).

However in cases (i) and (ii) the accuracy of the G–C formula decreases when r approaches the endpoints ± 1 or, that it is the same, the collocation point is near to a vertex of Γ, and q increases. The reason of this behaviour is due to the complex poles of the kernel function, whose distance from $(-1,1)$ depends on r and q. The more q is large and r is close to ± 1, the more these poles are close to $(-1,1)$ and make poor the approximations of the corresponding integrals. Nevertheless, in the numerical examples we have considered, this deterioration does not seem to affect the final accuracy of the (discrete) collocation method.

However, for completeness and to point out how the use of proper changes of variable may improve the performance of a quadrature rule, here we suggest a particular approach for computing the integrals in the above critical situations. To improve the accuracy of the G–C formula we suggest, before applying it, to introduce a preliminary change of variable, which allows to move away the complex poles from $(-1,1)$. Among all the possible choices, we have considered the following two simple and more practical changes of variable

$$\delta(\tau) = 1 - \frac{(1-\tau)^p}{2^{p-1}} \quad p \in \mathbb{N} \quad \tau \in [-1,1] \tag{21}$$

when in (15) r is close to 1 and $j=i$, or when r is close to -1 and $j=1$ and $i=l$ or $j=i+1$ (if $l>2$);

$$\delta(\tau) = -1 + \frac{(1+\tau)^p}{2^{p-1}} \quad p \in \mathbb{N} \quad \tau \in [-1,1] \tag{22}$$

when in (15) r is close to -1 and $j=i$, or when r is close to 1 and $j=l$ and $i=1$ or $j=i-1$ (if $l>2$). If $l=2$ then we use (21) ((22)) when r is close to 1 (-1) and $j=i$, or to -1 (1) and $j \neq i$. How close r must be to one of the endpoints to take advantage from the proposed changes of variable depends on the smoothing parameter q of γ: the larger q is, the larger the neighbourhood of ± 1 is. For example, for $q=3$ this approach gives better approximations than the G–C rule for values of r such that $(1 \pm r) \leqslant 10^{-1}$. This because the image of a point r, such that $(1 \pm r) \approx 10^{-k}$, under the smoothing parametrization α_i have a distance from the nearest endpoint of $(-1,1)$ which is of order 10^{-qk}. The smoothing transformation produces a knot concentration with exponent q in the neighbourhood of the endpoints ± 1.

Note that the above simple transformation does not change the interval of integration and $p=1$ means no change of variable. Introducing in (18) the change of variable $\rho = \delta(\tau)$ and setting $b(\tau) := c(1-\tau)$ or $b(\tau) := c(1+\tau)$, with

$$c(x) := \frac{p x^{\frac{p-1}{2}}}{\sqrt{2^{p-1} + 2^{p-2}x + \cdots + x^{p-1}}} \tag{23}$$

Table I. Relative errors $|I^S_{512} - I^S_m|/|I^S_{512}|$, with $j = i$.

$q=3$	$r=-0.9$		$r=-0.99$		$r=-0.999$		$r=-0.9999$	
m	$p=1$	$p=3$	$p=1$	$p=3$	$p=1$	$p=3$	$p=1$	$p=3$
4	$1.15-03$	$5.61-03$	$5.42-02$	$5.75-03$	$9.70-02$	$6.24-03$	$1.12-01$	$1.11-02$
8	$2.52-04$	$3.69-05$	$6.25-03$	$2.55-04$	$3.69-02$	$9.67-04$	$5.21-02$	$1.26-03$
16	$2.52-07$	$7.76-09$	$5.90-04$	$9.54-07$	$9.31-03$	$9.36-06$	$2.22-02$	$6.94-05$
32	$3.79-13$	—	$1.97-06$	$2.56-11$	$3.34-04$	$1.44-08$	$7.71-03$	$1.69-07$
64	—	—	$1.71-09$	—	$7.52-05$	—	$1.43-03$	$4.62-11$
128	—	—	—	—	$2.32-07$	—	$5.15-05$	—
256	—	—	—	—	$2.94-12$	—	$4.58-06$	—

according to the definition (21) or (22) of $\delta(\tau)$ respectively, the integral I^S becomes

$$I^S = -\frac{1}{\pi}\int_{-1}^{1} \log|\alpha_j(r) - \alpha_i(\delta(\tau))| \frac{T_{h-1}(\delta(\tau))\, b(\tau)}{\sqrt{1-\tau^2}}\, d\tau \tag{24}$$

We remark that the polynomial at the denominator of (23) admits only complex poles, which are farther from $(-1,1)$ than those of the log-kernel. As concerns these latters we have to remark that if on one hand the change of variable allows to move them away from $(-1,1)$, on the other hand their number increases as p becomes larger and larger and, therefore, some of them inevitably approach again the interval $(-1,1)$. However, it is sufficient to choose p not too large to obtain the full accuracy with a reasonable number of nodes (see, for instance, the tables below).

Finally, to compute I^S given by (24), we apply a G–C quadrature formula

$$I^S_m = -\frac{1}{m}\sum_{k=1}^{m} \log|\alpha_j(r) - \alpha_i(\delta(x_{m,k}))|\, T_{h-1}(\delta(x_{m,k}))\, b(x_{m,k})$$

with $x_{m,k}$, $k = 1,\ldots,m$, given by (13). In the evaluation of the log-kernel we have used the expression (18) or the approximations (19) or (20), with $\rho = \delta(x_{m,k})$.

In the following numerical tests we have chosen $h = 1$ and $q = 3$. To compare the numerical values obtained by applying an m-point G–C formula to the original integral (15) (or (24) with $p = 1$) and to the transformed one (24) with $p > 1$, we have considered as a significant example three consecutive corners P_{i-1}, P_i, P_{i+1} of a polygon Γ such that: the side joining P_{i-1} (P_i) to P_i (P_{i+1}) is Γ_{i-1} (Γ_i), the lengths $|\Gamma_{i-1}|$ and $|\Gamma_i|$ are both equal to 1 and the interior angle between Γ_{i-1} and Γ_i is β_i.

Then we have tested the numerical procedures with $p = 1$ and 3, for case (i) of (16) in Table I and for case (ii) in Table II. In this latter case the domain of integration is Γ_i and the collocation point belongs to Γ_{i-1}.

Moreover, we have chosen a fixed collocation point ($r = 0.99$) and three different values of β_i to point out that the accuracy of both procedures ($p = 1$ and 3) also depends sensitively on the interior angle between two sides or arcs of the boundary.

Finally, we remark that the numerical results are substantially similar when $\bar{\alpha}_i$ is not linear (Γ is not a polygon). Moreover, values of the exponent p higher than three produce negligible improvements.

Table II. Relative errors $|I^S_{512} - I^S_m|/|I^S_{512}|$, with $r = 0.99 \in \Gamma_j$ and $j = i - 1$.

$q=3$	$\beta_i = \pi/8$		$\beta_i = \pi/4$		$\beta_i = \pi/2$	
m	$p=1$	$p=3$	$p=1$	$p=3$	$p=1$	$p=3$
4	$1.01-01$	$2.72-02$	$9.81-02$	$2.44-02$	$9.41-02$	$2.02-02$
8	$4.10-03$	$7.21-03$	$5.18-03$	$5.00-03$	$4.54-03$	$2.51-03$
16	$2.19-03$	$2.51-03$	$4.35-05$	$1.74-03$	$2.26-03$	$5.32-04$
32	$7.49-03$	$3.53-04$	$3.63-03$	$1.45-04$	$8.73-04$	$1.66-05$
64	$1.26-03$	$1.51-04$	$3.52-04$	$1.12-05$	$1.15-05$	$4.12-08$
128	$1.99-05$	$7.27-07$	$5.24-06$	$1.33-08$	$2.22-07$	$1.80-12$
256	$1.28-05$	$2.59-08$	$1.02-07$	$8.54-13$	$6.61-12$	—

We have chosen as reference value that obtained with $m = 512$ quadrature nodes. All computations have been performed on a standard PC using 16-digit double precision arithmetic. The symbol – means that the corresponding approximation has achieved a full accuracy.

3. THE DIRICHLET–NEUMANN PROBLEM IN 2D

In this section we consider the following Dirichlet–Neumann problem for the Laplace equation

$$\begin{aligned} \Delta u &= 0 \quad \text{on } \Omega \\ u &= \bar{f} \quad \text{on } \Gamma_D = \bigcup_{i=1}^{l} \Gamma_i^D, \ l \geqslant 1 \\ \frac{\partial u}{\partial \mathbf{n}} &= \bar{g} \quad \text{on } \Gamma_N = \bigcup_{i=l+1}^{l+\bar{l}} \Gamma_i^N \end{aligned} \tag{25}$$

Let $\Gamma := \Gamma_D \cup \Gamma_N = \partial\Omega$. Using the single layer representation (2) of u we obtain (3), that is

$$-\frac{1}{\pi}\int_\Gamma \log|P-Q|\bar{z}(Q)\,\mathrm{d}S_Q = \bar{f}(P) \quad P \in \Gamma_D$$

$$\bar{z}(P) - \frac{1}{\pi}\int_\Gamma \frac{\partial \log|P-Q|}{\partial n_P}\bar{z}(Q)\,\mathrm{d}S_Q = \bar{g}(P) \quad P \in \Gamma_N$$

where the density function $\bar{z}$ is sought on Γ. Setting $\bar{z}_i := \bar{z}|_{\Gamma_i}$ and taking into account of the following behaviour of $\bar{z}$ near the corners P_i:

$$\bar{z}(P) = c(\theta) r^{s_i} + \text{smoother terms}, \quad s_i = \min\left\{\frac{\pi}{2\beta_i}, \frac{\pi}{2(2\pi-\beta_i)}\right\} - 1 \quad P \in \Gamma$$

where r, θ, β_i have been defined in Section 2, we proceed in a way similar to the previous one used for the Dirichlet problem. Therefore, after introducing the smoothing parametrization $\alpha_j(t) := \bar{\alpha}_j(\gamma((t+1)/2))$, $j = 1, \ldots, l + \bar{l}$, that is $\alpha_{h,j}(t) := \bar{\alpha}_{h,j}(\gamma((t+1)/2))$, $h = 1, 2$, and the

Chebyshev weight $w(x)$, and multiplying the second equation of the system by $|\alpha_j'(r)|\sqrt{1-r^2}$, finally we have to solve the following system of integral equations:

$$\begin{aligned} &-\frac{1}{\pi}\sum_{i=1}^{l+\bar{l}}\int_{-1}^{1}\log|\alpha_j(r)-\alpha_i(\rho)|\frac{z_i(\rho)}{\sqrt{1-\rho^2}}\,\mathrm{d}\rho = f_j(r) \quad j=1,\ldots,l,\ \ l\geqslant 1 \\ &z_j(r)-\frac{1}{\pi}\sqrt{1-r^2}\sum_{i=1}^{l+\bar{l}}\int_{-1}^{1}K_{j,i}(r,\rho)\frac{z_i(\rho)}{\sqrt{1-\rho^2}}\,\mathrm{d}\rho = g_j(r) \quad j=l+1,\ldots,l+\bar{l} \end{aligned} \tag{26}$$

where

$$z_i(\rho) := \bar{z}_i(\alpha_i(\rho))|\alpha_i'(\rho)|\sqrt{1-\rho^2}$$

$$f_j(r) := \bar{f}(\alpha_j(r)) \quad g_j(r) := \bar{g}(\alpha_j(r))|\alpha_j'(r)|\sqrt{1-r^2}$$

and

$$\begin{aligned} K_{j,i}(r,\rho) &:= K(\alpha_j(r),\alpha_i(\rho))|\alpha_j'(r)| \\ &= \frac{[\alpha_{2,j}'(r)(\alpha_{1,j}(r)-\alpha_{1,i}(\rho))]-[\alpha_{1,j}'(r)(\alpha_{2,j}(r)-\alpha_{2,i}(\rho))]}{(\alpha_{1,j}(r)-\alpha_{1,i}(\rho))^2+(\alpha_{2,j}(r)-\alpha_{2,i}(\rho))^2} \\ &=: \frac{B_1-B_2}{(\alpha_{1,j}(r)-\alpha_{1,i}(\rho))^2+(\alpha_{2,j}(r)-\alpha_{2,i}(\rho))^2} \end{aligned} \tag{27}$$

3.1. A Chebyshev collocation method

To solve numerically (26) we propose the following collocation method,

$$\begin{aligned} &-\frac{1}{\pi}\sum_{i=1}^{l+\bar{l}}\sum_{h=1}^{n}a_{(i-1)n+h}\int_{-1}^{1}\log|\alpha_j(x_{n,k})-\alpha_i(\rho)|\frac{T_{h-1}(\rho)}{\sqrt{1-\rho^2}}\,\mathrm{d}\rho = f_j(x_{n,k}) \\ &\quad k=1,\ldots,n \quad j=1,\ldots,l \quad l\geqslant 1 \\ &\sum_{h=1}^{n}a_{(j-1)n+h}T_{h-1}(x_{n,k})-\frac{1}{\pi}\sqrt{1-x_{n,k}^2}\sum_{i=1}^{l+\bar{l}}\sum_{h=1}^{n}a_{(i-1)n+h} \\ &\int_{-1}^{1}K_{j,i}(x_{n,k},\rho)\frac{T_{h-1}(\rho)}{\sqrt{1-\rho^2}}\,\mathrm{d}\rho = g_j(x_{n,k}) \quad k=1,\ldots,n \quad j=l+1,\ldots,l+\bar{l} \end{aligned} \tag{28}$$

where T_{h-1} and $x_{n,k}$ are defined at the beginning of Section 2.1.

To evaluate the matrix elements we have to compute (numerically) the integral I^S given by (15) and

$$\begin{aligned} &I^D := -\frac{1}{\pi}\int_{-1}^{1}K_{j,i}(r,\rho)\frac{T_{h-1}(\rho)}{\sqrt{1-\rho^2}}\,\mathrm{d}\rho \\ &\quad r := x_{n,k} \quad k,h=1,\ldots,n \quad i=1,\ldots,l+\bar{l} \quad j=l+1,\ldots,l+\bar{l} \end{aligned} \tag{29}$$

Table III. Relative errors $|I^D_{512} - I^D_m|/|I^D_{512}|$, with $r = -0.99 \in \Gamma_j$ and $j = i$.

	$K_{j,j}$ is given by (27)	$K_{j,j}$ is given by (31) with			
$q = 3$		$R_c(\bar{r}, \overline{\delta\tau}) = 0$		$R_c(\bar{r}, \overline{\delta\tau}) \neq 0$	
m	$p = 1$	$p = 1$	$p = 3$	$p = 1$	$p = 3$
4	5.62 − 04	5.64 − 04	1.81 − 02	1.65 − 02	4.44 − 02
8	4.55 − 06	6.86 − 06	5.84 − 04	3.90 − 04	2.81 − 03
16	1.61 − 06	4.87 − 11	3.53 − 07	2.25 − 07	1.14 − 05
32	7.67 − 06	—	—	1.21 − 11	2.62 − 10
64	6.23 − 07	—	—	6.87 − 11	1.10 − 10
128	8.39 − 07	—	—	3.99 − 12	7.90 − 11
256	4.54 − 04	—	—	2.17 − 11	1.03 − 10

with $K_{j,i}$ given by (27). As regards to I^S, we proceed as described in Section 2.1. To compute I^D we consider separately the three cases stated in (16).

Note that in case (i) if $\bar{\alpha}_j$ is linear, i.e. Γ_j consists of a straight line, then $K_{j,j} = 0$; otherwise we have that the kernel is at least continuous for $-1 < r, \rho < 1$, because

$$K_{j,j}(r,\rho) = \frac{1}{2}\frac{\alpha'_{1,j}(r)\alpha''_{2,j}(r) - \alpha'_{2,j}(r)\alpha''_{1,j}(r)}{[\alpha'_{1,j}(r)]^2 + [\alpha'_{2,j}(r)]^2} \quad \rho = r \tag{30}$$

Indeed, the degree of smoothness of $K_{j,j}$ is the same of the parametrization $\bar{\alpha}_j$ of Γ_j; taking into account that r is fixed and internal to $(-1,1)$ and assuming $\bar{\alpha}_j$ smooth in $[-1,1]$, $K_{j,j}$ turns out to be smooth for any $\rho \in [-1,1]$. Nevertheless when $j = i$ we need to use a more refined expression for the representation of the kernel $K_{j,j}$ to avoid numerical cancellation phenomena. Indeed, various and severe numerical cancellation phenomena occur in the evaluation of some quantities of the kernel $K_{j,j}$. In particular, leaving out those depending on the particular parametrization $\bar{\alpha}_j$, we will consider only those originated from the difference $\alpha_{c,j}(r) - \alpha_{c,j}(\rho)$, $c = 1,2$, which depends on the distance of $\bar{r} := \gamma((r+1)/2)$ from $\bar{\rho} := \gamma((\rho+1)/2)$, and from the difference $B_1 - B_2$ at the numerator of $K_{j,j}$ (see (27)). This latter, which produces a larger loss of accuracy, can be avoided by expanding the function $\bar{\alpha}_{c,j}$ in Taylor's series about the point $\bar{r}$. Indeed, we have

$$K_{j,j}(r,\rho) = \frac{-\alpha'_{2,j}(r)\left[\bar{\alpha}''_{1,j}(\bar{r})\frac{1}{2!} + R_1(\bar{r},\bar{\rho})\right] + \alpha'_{1,j}(r)\left[\bar{\alpha}''_{2,j}(\bar{r})\frac{1}{2!} + R_2(\bar{r},\bar{\rho})\right]}{[\bar{\alpha}'_{1,j}(\bar{r}) + \bar{\alpha}''_{1,j}(\bar{r})(\bar{\rho}-\bar{r})/2! + R_1(\bar{r},\bar{\rho})]^2 + [\bar{\alpha}'_{2,j}(\bar{r}) + \bar{\alpha}''_{2,j}(\bar{r})(\bar{\rho}-\bar{r})/2! + R_2(\bar{r},\bar{\rho})]^2} \tag{31}$$

with $R_c(\bar{r},\bar{\rho}) = \bar{\alpha}'''_{c,j}(\xi_c)(\bar{\rho}-\bar{r})/3!$, $|\xi_c - \bar{r}| \leqslant |\bar{\rho} - \bar{r}|$, $c = 1,2$. Note that if $\bar{\alpha}_j$ is a polynomial of low degree, for example of degree 2, then in (31) $R_c(\bar{r},\bar{\rho}) = 0$, $c = 1,2$, and we can obtain accurate approximations of the corresponding integral (see Table III) for low values of n with a little computational effort. Moreover, when the remainder $R_c(\bar{r},\bar{\rho})$ of the Taylor expansion is not zero and $\bar{r}$ is not close enough to $\bar{\rho}$, to obtain accurate numerical results we have to consider many terms of the expansion. Indeed, we may have B_1 and B_2 in (27) nearly equal, while the terms $\bar{r}$ and $\bar{\rho}$ are not close enough to produce a small remainder.

Table IV. Relative errors $|I^D_{512} - I^D_m|/|I^D_{512}|$, with $r = 0.99 \in \Gamma_j$ and $j = i - 1$.

$q=3$	$\beta_i = \pi/8$		$\beta_i = \pi/4$		$\beta_i = \pi/2$	
m	$p=1$	$p=3$	$p=1$	$p=3$	$p=1$	$p=3$
4	9.89 − 01	9.82 − 01	9.77 − 01	9.61 − 01	9.51 − 01	9.19 − 01
8	5.72 − 01	8.43 − 01	1.55 − 01	6.81 − 01	4.18 − 01	4.22 − 01
16	8.25 − 01	1.14 − 01	6.47 − 01	3.26 − 01	3.68 − 01	1.87 − 01
32	1.76 + 00	5.44 − 02	9.55 − 01	5.72 − 02	3.55 − 01	9.67 − 03
64	4.79 − 01	1.24 − 01	1.77 − 01	1.10 − 02	1.62 − 02	6.92 − 05
128	3.81 − 02	8.79 − 04	1.55 − 03	2.06 − 05	2.43 − 04	4.60 − 09
256	1.96 − 02	8.47 − 05	1.88 − 04	3.31 − 09	1.15 − 08	—

Taking into account the above remarks, in case (i) of (16) to compute (29) we have applied a G–C rule and we have used the representation (30) of $K_{j,j}$ when $|\rho - r| \leqslant eps$, (31) or its approximation with R_c omitted when $|\bar{\rho} - \bar{r}| \leqslant eps$, or (27) in the remaining cases.

In cases (ii) and (iii) we have computed (29) by using (27) and a G–C quadrature formula.

However, as for I^S in (17), in cases (i) and (ii) $K_{i,j}$ admits complex poles located on circles centered in ± 1, such that the more r is close to ± 1 and q is large, the more some of these poles are close to the interval of integration. Therefore, also in these cases, to improve the numerical computation of the integral (29) by means of a G–C quadrature rule, we suggest the introduction in (27) of the change of variable (21) or (22) (according to the closeness of r to -1 or 1, respectively), which gives

$$I^D = -\frac{1}{\pi}\int_{-1}^{1} K_{j,i}(r, \delta(\tau))\frac{T_{h-1}(\delta(\tau))b(\tau)}{\sqrt{1-\tau^2}}\,\mathrm{d}\tau \tag{32}$$

Nevertheless, when $j = i$ the choice $p > 1$ in (21) or (22) is not so efficient as $p = 1$: the results for $p = 1$ are better than those for $p = 3$ for moderate values of n. This because the transformation $\delta(\tau)$ with $p > 1$, moving further the quadrature nodes towards the endpoint ± 1 closest to the collocation point $\bar{r}$, causes a larger loss of significant digits in the computation of $\overline{\delta\tau} - \bar{r}$, where $\overline{\delta\tau} := \gamma((\delta(\tau) + 1)/2)$.

In Table III we have reported the relative errors obtained by applying an m-point G–C quadrature formula to the integral (32), with $r = -0.99$ and $q = 3$. We have compared the numerical results obtained by using for the kernel $K_{j,j}$ expressions (27) and (31) with $\rho = \delta(\tau)$. In expressions (27) and (31) with $R_c(\bar{r}, \overline{\delta\tau}) = 0$, $\bar{\alpha}_j$ is the parametrization of the arc of parabola $y = x - x^2$, $x \in [0, 1]$, oriented counter-clockwise. Comparing the results for $p = 1$ reported in the second and in the third column, we can see how the numerical cancellation disappears by using Taylor's expansion. In the last four columns we use for $K_{j,j}$ expression (31) where $\bar{\alpha}_j$ is defined by a trigonometric expression and the expansion is truncated to the terms of the third order, i.e. $R_c(\bar{r}, \overline{\delta\tau}) \neq 0$, $c = 1, 2$ is omitted.

Since in case (ii) we have no numerical cancellation phenomenon, the change of variable $\delta(\tau)$ with $p > 1$ is efficient. Indeed, the numerical results obtained with $p = 3$ are better than those with $p = 1$ for values of n bigger than 32 (see Table IV). In Table IV the arcs $\Gamma_j = \Gamma_{i-1}$ and Γ_i are the same considered in Table II.

4. NUMERICAL TESTS

In this section we apply the collocation methods proposed in Sections 2 and 3 to solve some significant test problems. We first consider Dirichlet problems and then the Neumann–Dirichlet ones.

As already remarked in Section 2, in the implementation of our collocation method, to evaluate the integrals of the linear collocation system we have used the G–C quadrature rule, with a number of quadrature nodes which is twice that of the collocation nodes. Indeed, when solving integral equations with our numerical approach, the final numerical results obtained by using the quadrature rules proposed in Sections 2.1 and 3.1 are only a little better than those obtained by using directly a G–C quadrature rule. This because a very good accuracy is achieved already by low values of the degree of the local approximant polynomial (hence, of the number n of the collocation nodes) and of the smoothing exponent q of γ. Therefore, for the values of n and q considered, the transformation $\delta(\tau)$ with $p>1$ does not perform better than the G–C quadrature rule ($p=1$) because the points $r \equiv x_{n,k}$ are not very close to ± 1. Moreover, when solving integral equations by a collocation method, for low and fixed values of n it is not necessary to compute the integrals up to the machine precision, since the global error seems to be determined mainly by that of the collocation method. In practice, the accuracy does not vary substantially if we evaluate the integrals with $m=2n$ Chebyshev quadrature nodes, or for example $m=4n$ or $2n$ and using the smoothing change of variable when r is close to ± 1.

Since our goal is the computation of the solution $u(P)$ of the boundary value problems (4) and (25), from the single layer representation (2) of the potential, introducing the smoothing parametrization $\alpha_i(\rho)$ and using the notation (11) we get

$$u(P) = -\frac{1}{\pi}\sum_i \int_{\Gamma_i} \log|P-Q|\bar{z}_i(Q)\,\mathrm{d}S_Q = -\frac{1}{\pi}\sum_i \int_{-1}^{1} \log|P-\alpha_i(\rho)|\frac{z_i(\rho)}{\sqrt{1-\rho^2}}\,\mathrm{d}\rho \tag{33}$$

where z_i is solution of (10) or (26).

To test in a meaningful way our approach, the point P has been chosen close to a corner of the boundary, either inside or outside Ω, since this is considered the difficult situation. In particular, we have computed the relative errors $|u(P)-u_n(P)|/|u(P)|$, where in the chosen examples u is known a priori in Ω and u_n is the analogue of (33), but with z_i replaced by $z_{i,n}$ (see (12)). Outside Ω we have used $u_{\bar{n}}$, generally with $\bar{n}=128$, as reference value. The integrals (33) with $z_{i,n}$ instead of z_i have been computed by means of a G–C quadrature rule with $\bar{m}=256$ nodes, i.e.

$$u_n(P) = -\frac{1}{\pi}\sum_i \int_{-1}^{1} \log|P-\alpha_i(\rho)|\frac{z_{i,n}(\rho)}{\sqrt{1-\rho^2}}\,\mathrm{d}\rho$$

$$\sim -\frac{1}{\bar{m}}\sum_i \sum_{h=1}^{n} a_{(i-1)n+h} \sum_{r=1}^{\bar{m}} \log|P-\alpha_i(x_{\bar{m},r})|T_{h-1}(x_{\bar{m},r})$$

Moreover, setting

$$M_z := \int_\Gamma \bar{z}(Q)\,\mathrm{d}S_Q = \sum_i \int_{\Gamma_i} \bar{z}_i(Q)\,\mathrm{d}S_Q = \sum_i \int_{-1}^{1} \frac{z_i(\rho)}{\sqrt{1-\rho^2}}\,\mathrm{d}\rho$$

for each example, we have also computed the following approximated values

$$M_{z_n} = \sum_i \int_{-1}^{1} \frac{z_{i,n}(\rho)}{\sqrt{1-\rho^2}}\,\mathrm{d}\rho = \sum_i \sum_{h=1}^{n} a_{(i-1)n+h} \int_{-1}^{1} \frac{T_{h-1}(\rho)}{\sqrt{1-\rho^2}}\,\mathrm{d}\rho = \pi \sum_i a_{(i-1)n+1}$$

and reported in the following tables the relative errors $|M_{z_{\bar{n}}} - M_{z_n}|/|M_{z_{\bar{n}}}|$, with $M_{z_{\bar{n}}}$ as reference value.

In the following figures of boundaries, the Dirichlet and Neumann arcs have been denoted by the capital letters D and N, respectively. Moreover, the symbol $+$ points out the position of the point P in which potential (33) has been computed.

In each of the following tables we have reported the numerical results for the values of $n = 8, 16, 32, 64$, where $n-1$ is the local degree of the approximant polynomial, and for the values $q = 1, 2, 3$, where $q = 1$ means that the smoothing technique has not been applied. We remark that $q = 3$ may be considered as the 'optimal' smoothing parameter, because it allows us to get an accuracy which is twice that obtained with $q = 1$ for the same value of $n = 64$. Note that $q = 2$ needs values of n larger than 64 to get that accuracy. The same remark is valid for $q > 3$, because of the growing flatness of γ due to the increasing of q. In this latter case the accuracy improves only for large values of n.

Finally, we remark that the choices $q = 1$ and $q > 1$ lead to the same computational cost; the smoothing technique requires only negligible additional computational efforts. Moreover, in the case of a Dirichlet problem and if the parametrization of the boundary is odd or even, the computational time may be halved by taking advantage of the properties that γ is an odd function, T_j is odd if j is odd and is even if j is even, and the symmetric distribution in $(-1, 1)$ of the quadrature and collocation nodes, both coinciding with the zeros of the Chebyshev polynomials of the first kind.

To conclude with a general practical rule, when solving integral equations by means of a discrete collocation method, we suggest to choose $q = 3$ in (7) and $p = 1$ in (21) or (22). This latter implies the use of a G–C rule to compute the collocation matrix elements.

Test 1

As first test we have solved a Dirichlet problem on a domain Ω with an 'L-shaped' boundary (see Figure 1).

To choose *a priori* a known solution u which has a realistic behaviour near the corners, we have taken as solution of (4) the function

$$u(x, y) = Re(\xi^{2/3}) = r^{2/3} \cos\frac{2\theta}{3} \quad \xi = x + iy = r\mathrm{e}^{\mathrm{i}\theta} \quad (x, y) \in \Re^2 \backslash (0, 0)$$

Because u is the real part of an analytic function, u satisfies the Laplace equation in Ω. Setting $u =: \bar{f}$ on Γ, we have solved the corresponding system of integral equations (14). The numerical results are reported in Tables V and VI.

Test 2

As second example we have employed a domain formed by four circular arcs, centred at ± 1 and ± 3, respectively, and each of radius 3.64 (see Figure 2).

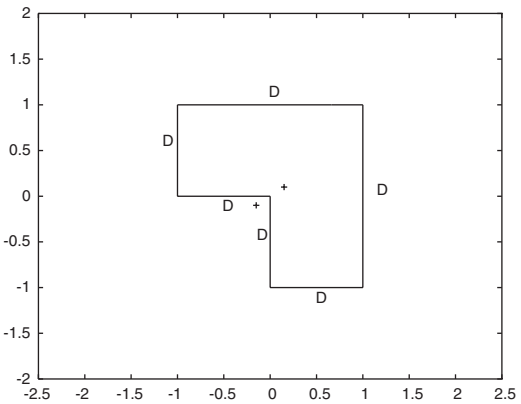

Figure 1. The contour Γ in Test 1.

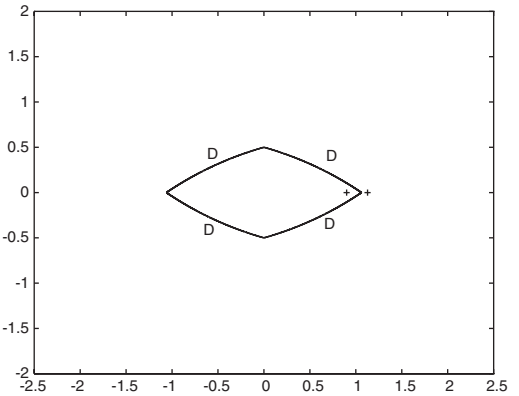

Figure 2. The contour Γ in Test 2.

Table V. Relative errors in Test 1.

	$\lvert u(P)-u_n(P)\rvert/\lvert u(P)\rvert$ at $P=(0.15,0.1)$			$\lvert u_{128}(P)-u_n(P)\rvert/\lvert u_{128}(P)\rvert$ at $P=(-0.15,-0.1)$		
n	$q=1$	$q=2$	$q=3$	$q=1$	$q=2$	$q=3$
8	$2.77-04$	$2.77-05$	$6.54-05$	$8.64-03$	$1.15-03$	$1.64-02$
16	$4.48-05$	$1.13-07$	$9.50-08$	$4.74-04$	$1.06-05$	$1.81-05$
32	$7.15-06$	$1.95-09$	$7.50-10$	$6.50-05$	$1.08-07$	$1.35-08$
64	$1.13-06$	$3.97-11$	$3.31-12$	$1.03-05$	$1.71-09$	$1.25-11$

Table VI. Relative errors in Test 1.

	$\lvert M_{z_{128}}-M_{z_n}\rvert/\lvert M_{z_{128}}\rvert$		
n	$q=1$	$q=2$	$q=3$
8	$7.45-04$	$4.82-05$	$1.34-05$
16	$1.19-04$	$1.00-06$	$1.22-07$
32	$1.88-05$	$2.34-08$	$6.83-10$
64	$2.96-06$	$5.73-10$	$3.00-12$

The potential u assumed over the above domain is

$$u(x,y)=\log[(x-2)^2+(y-2)^2]^{-0.5}+x^2-y^2$$

which is harmonic in $\Re^2$. The results obtained by the method here proposed for the problem (4) with $u=:\bar{f}$ on Γ are reported in Tables VII and VIII.

Test 3

To test our numerical approach we have also chosen a domain with a cut; in particular, we have considered a square of unit side with a cut defined by $\frac{1}{3}\leqslant x\leqslant\frac{2}{3}$ and $y=\frac{1}{3}$ (see Figure 3).

Table VII. Relative errors in Test 2.

	$\lvert u(P)-u_n(P)\rvert/\lvert u(P)\rvert$ at $P=(0.9,0)$			$\lvert u_{128}(P)-u_n(P)\rvert/\lvert u_{128}(P)\rvert$ at $P=(1.1,0)$		
n	$q=1$	$q=2$	$q=3$	$q=1$	$q=2$	$q=3$
8	$3.24-03$	$3.82-04$	$1.64-02$	$1.26-03$	$8.83-05$	$1.52-04$
16	$5.24-05$	$5.55-05$	$2.16-06$	$1.87-04$	$1.06-06$	$1.94-06$
32	$4.19-08$	$1.35-07$	$2.18-08$	$3.22-05$	$4.50-08$	$1.77-08$
64	$1.08-08$	$2.11-11$	$2.22-12$	$5.78-06$	$1.56-09$	$1.18-10$

Table VIII. Relative errors in Test 2.

	$\lvert M_{z_{128}}-M_{z_n}\rvert/\lvert M_{z_{128}}\rvert$		
n	$q=1$	$q=2$	$q=3$
8	$8.09-05$	$4.44-06$	$2.44-06$
16	$9.64-06$	$1.67-09$	$5.15-08$
32	$1.31-06$	$9.90-10$	$4.71-10$
64	$1.97-07$	$3.96-11$	$3.14-12$

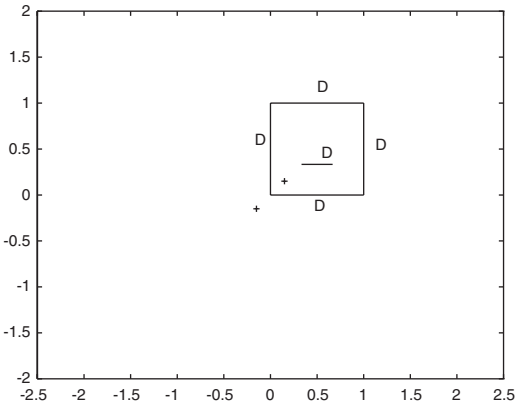

Figure 3. The contour Γ in Test 3.

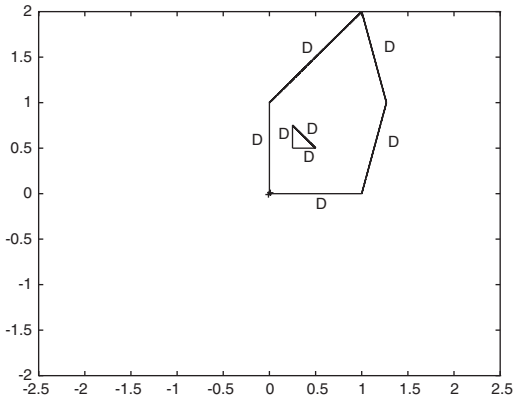

Figure 4. The contour Γ in Test 4.

The potential u assumed on this domain is

$$u(x,y)=\sin(x)\cosh(y)$$

and the results corresponding to problem (4) with $u=:\bar{f}$ on Γ are reported in Tables IX and X.

Test 4

The last domain, on which we have tested our numerical approach for the resolution of problem (4), is a polygon with corners of varying angles and with a triangular hole inside (see

Table IX. Relative errors in Test 3.

	$\lvert u(P)-u_n(P)\rvert/\lvert u(P)\rvert$ at $P=(0.15,0.15)$			$\lvert u_{128}(P)-u_n(P)\rvert/\lvert u_{128}(P)\rvert$ at $P=(-0.15,-0.15)$		
n	$q=1$	$q=2$	$q=3$	$q=1$	$q=2$	$q=3$
8	7.54 − 05	2.14 − 05	5.41 − 04	1.33 − 04	4.72 − 06	2.27 − 06
16	1.18 − 07	6.26 − 08	2.17 − 07	2.10 − 05	4.34 − 08	6.20 − 08
32	3.69 − 09	1.05 − 10	8.07 − 11	3.30 − 06	7.85 − 10	3.46 − 10
64	9.16 − 11	8.45 − 15	8.82 − 15	5.20 − 07	1.76 − 11	1.50 − 12

Table X. Relative errors in Test 3.

	$\lvert M_{z_{128}}-M_{z_n}\rvert/\lvert M_{z_{128}}\rvert$		
n	$q=1$	$q=2$	$q=3$
8	1.75 − 04	5.22 − 06	7.84 − 06
16	2.79 − 05	6.56 − 08	8.36 − 08
32	4.41 − 06	1.10 − 09	4.63 − 10
64	6.95 − 07	2.39 − 11	2.00 − 12

Table XI. Relative errors in Test 4.

	$\lvert u(P)-u_n(P)\rvert/\lvert u(P)\rvert$ at $P=(0.01,0.01)$			$\lvert u_{100}(P)-u_n(P)\rvert/\lvert u_{100}(P)\rvert$ at $P=(-0.01,-0.01)$		
n	$q=1$	$q=2$	$q=3$	$q=1$	$q=2$	$q=3$
8	1.33 − 03	3.06 − 04	2.62 − 04	5.68 − 03	2.50 − 04	1.45 − 04
16	8.86 − 04	3.81 − 06	1.16 − 07	5.69 − 04	8.66 − 08	1.53 − 06
32	1.94 − 05	8.80 − 08	1.30 − 08	6.90 − 05	1.61 − 08	7.19 − 09
64	3.89 − 08	2.60 − 11	7.34 − 12	1.07 − 05	3.55 − 10	3.10 − 11

Figure 4). More precisely, starting from the corner in $(0,0)$ and proceeding counter-clockwise, we have the following interior angles: $\frac{7}{12}\pi$, $\frac{5}{6}\pi$, $\frac{1}{3}\pi$, $\frac{3}{4}\pi$ and, at last, $\frac{1}{2}\pi$; the internal triangle has the right-angle in $(\frac{1}{2},\frac{1}{2})$, and two equal sides of size $\frac{1}{6}$.

As potential u in Ω we have chosen the harmonic function

$$u(x,y)=\mathrm{e}^x\cos(y)$$

and in Tables XI and XII we have reported the numerical results obtained solving the problem (4) with $u=:\bar{f}$ on the boundary of the domain given in Figure 4.

In the last two tests we consider the problem (25) on domains already defined in the tests 1 and 2, respectively.

Table XII. Relative errors in Test 4.

	$\lvert M_{z_{100}} - M_{z_n}\rvert / \lvert M_{z_{100}}\rvert$		
n	$q=1$	$q=2$	$q=3$
8	$1.39-04$	$2.21-06$	$9.65-06$
16	$2.49-05$	$4.78-08$	$6.32-08$
32	$4.25-06$	$1.72-09$	$4.34-11$
64	$7.16-07$	$6.13-11$	$1.51-12$

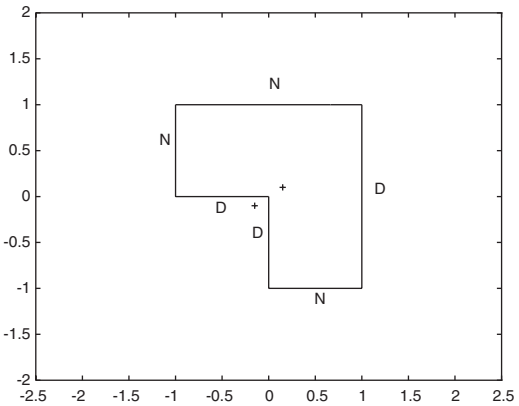

Figure 5. The contour Γ in Test 5.

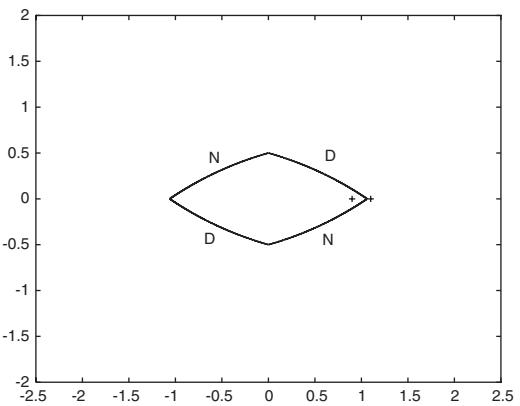

Figure 6. The contour Γ in Test 6.

Test 5

As in Test 1 we have first chosen a solution u of problem (25) which has a realistic behaviour at the corners of the domain in Figure 5.

Therefore, we have taken as solution of (25) the function

$$u(x,y)=Re(\xi^{1/3})=r^{1/3}\cos\frac{\theta}{3},\quad \xi=x+iy=re^{i\theta},\quad (x,y)\in\Re^2\backslash(0,0)$$

Then we have solved problem (25) with $u=:\bar{f}$ on Γ_D and $\partial u/\partial\mathbf{n}=:\bar{g}$ on Γ_N, where Γ_D and Γ_N denote the union of the arcs D and N, respectively (see Figure 5). The corresponding numerical results are reported in Tables XIII and XIV.

Test 6

As final test we have considered the curvilinear polygon defined in Test 2 and solved the problem (25) assuming the Dirichlet and Neumann data in such a way the solution of (25) in Ω (see Figure 6) is the harmonic function

$$u(x,y)=x^2-y^2$$

Table XIII. Relative errors in Test 5.

	$\lvert u(P)-u_n(P)\rvert/\lvert u(P)\rvert$ at $P=(0.15,0.1)$			$\lvert u_{128}(P)-u_n(P)\rvert/\lvert u_{128}(P)\rvert$ at $P=(-0.15,-0.1)$		
n	$q=1$	$q=2$	$q=3$	$q=1$	$q=2$	$q=3$
8	5.08 − 03	1.22 − 03	6.06 − 05	6.26 − 03	1.25 − 03	6.95 − 04
16	2.42 − 03	1.79 − 04	1.51 − 04	2.55 − 03	1.63 − 04	1.88 − 05
32	1.03 − 03	2.75 − 05	1.28 − 05	1.01 − 03	2.46 − 05	1.16 − 06
64	4.25 − 04	4.29 − 06	8.63 − 08	4.02 − 04	3.85 − 06	7.24 − 08

Table XIV. Relative errors in Test 5.

	$\lvert M_{z_{128}}-M_{z_n}\rvert/\lvert M_{z_{128}}\rvert$		
n	$q=1$	$q=2$	$q=3$
8	2.69 − 02	4.63 − 03	4.85 − 05
16	1.07 − 02	6.65 − 04	5.36 − 05
32	4.23 − 03	1.02 − 04	4.74 − 06
64	1.68 − 03	1.61 − 05	3.02 − 07

Table XV. Relative errors in Test 6.

	$\lvert u(P)-u_n(P)\rvert/\lvert u(P)\rvert$ at $P=(0.9,0)$			$\lvert u_{128}(P)-u_n(P)\rvert/\lvert u_{128}(P)\rvert$ at $P=(1.1,0)$		
n	$q=1$	$q=2$	$q=3$	$q=1$	$q=2$	$q=3$
8	2.44 − 04	6.01 − 05	4.11 − 04	3.30 − 03	7.69 − 04	2.44 − 04
16	3.54 − 05	4.76 − 06	6.41 − 07	3.40 − 04	2.69 − 05	1.05 − 05
32	2.47 − 06	9.41 − 09	1.81 − 09	4.09 − 05	9.91 − 07	1.32 − 07
64	1.71 − 07	1.48 − 11	6.51 − 13	5.96 − 06	3.31 − 08	9.55 − 10

Table XVI. Relative errors in Test 6.

	$\lvert M_{z_{128}}-M_{z_n}\rvert/\lvert M_{z_{128}}\rvert$		
n	$q=1$	$q=2$	$q=3$
8	2.24 − 04	2.43 − 04	1.55 − 05
16	4.30 − 05	9.09 − 06	3.93 − 06
32	8.02 − 06	3.12 − 07	4.18 − 08
64	1.48 − 06	1.03 − 08	2.95 − 10

Therefore, using the following data $u =: \bar{f}$ on Γ_D and $\partial u/\partial \mathbf{n} =: \bar{g}$ on Γ_N, we have obtained the results of Tables XV and XVI.

5. THE DIRICHLET PROBLEM IN 3D

Here, we consider the Dirichlet problem for the Laplace equation

$$\begin{aligned} \Delta u &= 0 \quad \text{on } \Omega \\ u &= \bar{f} \quad \text{on } S = \bigcup_{i=1}^{l} S_i \end{aligned} \tag{34}$$

in a simply connected region Ω with piecewise smooth boundary S. Using the single layer representation of u,

$$u(A) = \int_S \frac{\psi(Q)}{|P-Q|}\, \mathrm{d}S_Q \quad A \in \Omega$$

we will look for the density function ψ which satisfies the following first kind BIE

$$\int_S \frac{\psi(Q)}{|P-Q|}\, \mathrm{d}S_Q = \bar{f}(P) \quad P \in S \tag{35}$$

or, equivalently,

$$\sum_{i=1}^{l} \int_{S_i} \frac{\psi_i(Q)}{|P-Q|}\, \mathrm{d}S_Q = \bar{f}(P) \tag{36}$$

where the unknowns $\psi_i := \psi|S_i$ are sought on S_i, $i = 1, \ldots, l$. We assume that each S_i is the continuous image of a polygonal region in the plane:

$$F_i : R_i \xrightarrow[\text{onto}]{1\text{-}1} S_i \quad i = 1, \ldots, l$$

Hence, by proceeding in the usual way (see Reference [1]), we create a (minimum) triangulation for S by first subdividing each R_j into a minimum number of triangles and then mapping this triangulation onto S_i. Therefore, starting from a triangulation of R_i, $\{\hat{\Delta}_{i,k}\colon\ k = 1, \ldots, n_i\}$, we define

$$\Delta_{i,k} := F_i(\hat{\Delta}_{i,k}) \quad k = 1, \ldots, n_i \quad i = 1, \ldots, l$$

Denoting by $T_{\bar{l}} = \{\Delta_1, \ldots, \Delta_{\bar{l}}\}$ the triangulation of S, we assume that $T_{\bar{l}}$ is a conforming triangulation, according to the definition given in Reference [1, p. 188]. Let $\{\hat{v}_{i,1}, \hat{v}_{i,2}, \hat{v}_{i,3}\}$ be the vertices of $\hat{\Delta}_i \subset R_j$, $i = 1, \ldots, \bar{l}$, $j = 1, \ldots, l$, such that $\Delta_i = F_j(\hat{\Delta}_i) \in T_{\bar{l}}$ and

$$U = \{(t_1, t_2)\colon\ 0 \leqslant t_1 \leqslant 1,\ t_1 + t_2 \leqslant 1\}$$

be the reference triangle. Using the affine mapping $G_i : U \xrightarrow[\text{onto}]{1\text{-}1} \hat{\Delta}_i$, given by

$$G_i(t_1, t_2) = u\hat{v}_{i,1} + t_2\hat{v}_{i,2} + t_1\hat{v}_{i,3} \quad u = 1 - t_1 - t_2 \tag{37}$$

we define the parametrization mapping $m_i : U \to \Delta_i$ as $m_i(t_1, t_2) = F_j(G_i(t_1, t_2))$ and we rewrite equation (36) in the following form:

$$\sum_{i=1}^{\bar{l}} \int_U \frac{\bar{\psi}_i(\tau_1, \tau_2)\, \mathrm{d}U}{|m_k(t_1, t_2) - m_i(\tau_1, \tau_2)|} = \bar{f}(m_k(t_1, t_2)) \quad k = 1, \ldots, \bar{l} \quad (t_1, t_2) \in U \tag{38}$$

where $\bar{\psi}_i(t_1, t_2) = \psi(m_i(t_1, t_2))|D_{t_1} m_i \times D_{t_2} m_i|$. As in the case of BIE on 2D domains, to improve the smoothness of the solution we introduce a polynomial smoothing transformation, which we derive from the one used in the interval case. To this aim we first introduce in (38) the Duffy transformation

$$D : (r_1, r_2) \in [0, 1] \times [0, 1] \to ((1 - r_2) r_1, r_1 r_2) \in U \tag{39}$$

which changes the reference triangle into the unit square $[0, 1] \times [0, 1]$. Hence, we have

$$\sum_{i=1}^{\bar{l}} \int_0^1 \int_0^1 \frac{\bar{z}_i(\rho_1, \rho_2)\, \mathrm{d}\rho_1\, \mathrm{d}\rho_2}{|\bar{\alpha}_k(r_1, r_2) - \bar{\alpha}_i(\rho_1, \rho_2)|} = \bar{f}(\bar{\alpha}_k(r_1, r_2)) \quad k = 1, \ldots, \bar{l} \quad 0 \leqslant r_1, r_2 \leqslant 1 \tag{40}$$

where

$$\bar{\alpha}_i(\rho_1, \rho_2) = m_i(D(\rho_1, \rho_2)) \quad \bar{z}_i(\rho_1, \rho_2) = \rho_1 \bar{\psi}_i(D(\rho_1, \rho_2)) \quad i = 1, \ldots, \bar{l}$$

We explicitly note that for some particular domains, such as, for example, cubes, L-blocks, cones or cylinders, we may consider directly a parametrization (eventually, the spherical co-ordinates) defined in a square, thus avoiding the introduction of the Duffy transformation.

As smoothing transformation we consider a polynomial function which is a little bit more general than the γ defined in (7). Indeed, we consider the following function:

$$\bar{\gamma}(t) = \frac{\int_0^t x^{q_1 - 1}(1 - x)^{q_2 - 1}\, \mathrm{d}x}{\int_0^1 x^{q_1 - 1}(1 - x)^{q_2 - 1}\, \mathrm{d}x} \quad q_1, q_2 \geqslant 1 \quad t \in [0, 1] \tag{41}$$

which satisfies properties analogous to γ, but has smoothing exponents q_1, q_2 which may be distinct and are not necessarily strictly greater than 1. This latter condition is assumed only when one needs to introduce a smoothing effect on the corresponding side of the square.

Introducing the smoothing transformation (41) in (40) and mapping $[0, 1]$ onto $[-1, 1]$ we get

$$\sum_{i=1}^{\bar{l}} \int_{-1}^1 \int_{-1}^1 \frac{z_i(\sigma_1, \sigma_2)\, \mathrm{d}\sigma_1\, \mathrm{d}\sigma_2}{|\alpha_k(s_1, s_2) - \alpha_i(\sigma_1, \sigma_2)|} = \bar{f}_k(s_1, s_2) \quad k = 1, \ldots, \bar{l} \quad -1 \leqslant s_1, s_2 \leqslant 1 \tag{42}$$

where

$$\alpha_i(\sigma_1, \sigma_2) = \bar{\alpha}_i\left(\bar{\gamma}\left(\frac{\sigma_1 + 1}{2}\right), \bar{\gamma}\left(\frac{\sigma_2 + 1}{2}\right)\right)$$

$$z_i(\sigma_1, \sigma_2) = \frac{1}{4}\bar{z}_i\left(\bar{\gamma}\left(\frac{\sigma_1 + 1}{2}\right), \bar{\gamma}\left(\frac{\sigma_2 + 1}{2}\right)\right)\bar{\gamma}'\left(\frac{s_1 + 1}{2}\right)\bar{\gamma}'\left(\frac{s_2 + 1}{2}\right)$$

$$f_k(s_1, s_2) = \bar{f}(\alpha_k(s_1, s_2))$$

To solve numerically (42) we have applied a collocation method, which for simplicity uses Legendre orthogonal expansions as approximant of the unknown functions z_i on each surface, and the zeros of Legendre polynomials as collocation node co-ordinates. Therefore, using the following polynomial approximation:

$$z_i(s_1,s_2)\sim z_{i,n}(s_1,s_2)=\sum_{h=1}^{n}\sum_{k=1}^{n}a_{(i-1)n^2+(h-1)n+k}P_{h-1}(s_1)P_{k-1}(s_2)\quad i=1,\ldots,\bar{l}$$

where P_r is the orthogonal Legendre polynomial of degree r, and the zeros $\xi_{n,k}$, $k=1,\ldots,n$, of P_n as co-ordinates of the collocation points, the final collocation linear system of $n\times n\times\bar{l}$ equations is

$$\begin{aligned}&\sum_{i=1}^{\bar{l}}\sum_{h=1}^{n}\sum_{k=1}^{n}a_{(i-1)n^2+(h-1)n+k}\int_{-1}^{1}\int_{-1}^{1}\frac{P_{h-1}(\sigma_1)P_{k-1}(\sigma_2)}{|\alpha_k(\xi_{n,u},\xi_{n,v})-\alpha_i(\sigma_1,\sigma_2)|}\,\mathrm{d}\sigma_1\,\mathrm{d}\sigma_2\\&\quad=f_k(\alpha_j(\xi_{n,u},\xi_{n,v}))\quad k=1,\ldots,\bar{l}\quad u,v=1,\ldots,n\end{aligned}\tag{43}$$

Unlike the bidimensional case, in the literature there are no available theoretical results on the stability and the convergence of collocation methods for solving the problem we are considering. Nevertheless, as the numerical results in Table XXI show, our collocation method seems to be very promising.

To evaluate the matrix elements in (43) we have to compute (numerically) the integral

$$\begin{aligned}&I:=\int_{-1}^{1}\int_{-1}^{1}\frac{g(\sigma_1,\sigma_2)}{|\alpha_k(s_1,s_2)-\alpha_i(\sigma_1,\sigma_2)|}\,\mathrm{d}\sigma_1\,\mathrm{d}\sigma_2\\&g(\sigma_1,\sigma_2)=P_{h-1}(\sigma_1)P_{k-1}(\sigma_2)\quad s_1:=\xi_{n,u},\quad s_2:=\xi_{n,v},\quad u,v=1,\ldots,n;\ j,i=1,\ldots,\bar{l}\end{aligned}\tag{44}$$

To this end we suggest different procedures of integration according to the values of i and k, and to the position of the collocation point $P\equiv\alpha_k(s_1,s_2)\in\Delta_k$, with respect to the (triangular) domain of integration Δ_i. The collocation point may belong to Δ_i or not. In the first case ($i=k$) the corresponding integral has a weak singularity at $P\equiv Q\equiv\alpha_i(\sigma_1,\sigma_2)$; in the second case ($P\notin\Delta_i$) the integrand is non-singular, but it becomes increasingly 'ill-behaved' as the distance between P and Δ_i decreases towards zero. For this reason, these integrals are referred as 'nearly singular integral'. In contrast, if P is not close to Δ_i, the integrands is quite well-behaved and a simple and standard quadrature method gives excellent accuracy.

We proceed to examine the cases separately and for each of them we describe the numerical procedure we have adopted. We first assume that the singularity P is in the interior of Δ_i; this implies that (s_1,s_2) is internal to the square $[-1,1]\times[-1,1]$. In this case we consider the partition of four triangles obtained joining the corners of the square with (s_1,s_2). Then, we split the integral over the square into a sum of four integrals, one for each of these triangles, and we map these latters to the reference triangle U by means of the affine mapping (37). Therefore, we have to deal with the integral below

$$I=\sum_{l=1}^{4}\int_{U}\frac{g(G_l(\tau_1,\tau_2))\,\mathrm{d}\tau_1\,\mathrm{d}\tau_2}{|\alpha_i(s_1,s_2)-\alpha_i(G_l(\tau_1,\tau_2))|}\tag{45}$$

Table XVII. Relative errors $|Q_{\bar{m}_1,\bar{m}_2} - Q_{m_1,m_2}|/|Q_{\bar{m}_1,\bar{m}_2}|$ for the integral (47) with $m_1 = \bar{m}_1 = 2$, $\bar{m}_2 = 256$.

m_2	$s_1 = s_2 = 0$	$s_1 = s_2 = 0.5$	$s_1 = s_2 = 0.9$	$s_1 = s_2 = 0.99$	$s_1 = s_2 = 0.999$	$s_1 = 0.999$ $s_2 = 0$
4	$3.93 - 04$	$2.13 - 03$	$2.65 - 02$	$1.36 - 02$	$2.81 - 03$	$1.72 - 03$
8	$2.51 - 07$	$9.00 - 06$	$2.58 - 03$	$3.67 - 03$	$2.07 - 03$	$1.40 - 03$
16	$1.39 - 13$	$3.08 - 09$	$5.94 - 05$	$1.97 - 03$	$1.20 - 03$	$1.13 - 03$
32	—	—	$5.76 - 08$	$1.52 - 04$	$7.86 - 07$	$8.45 - 04$
64	—	—	—	$2.31 - 06$	$3.27 - 05$	$5.61 - 04$
128	—	—	—	$2.79 - 10$	$1.61 - 06$	$2.78 - 04$

which has a weak singularity in $(0,0)$. To remove this latter we use the Duffy transformation (39) and, hence, we approximate the resulting integral by means of a standard product of Gauss–Legendre quadrature rules. At the end, from (39) and (45) we get

$$I \approx \sum_{l=1}^{4} \sum_{i=1}^{m_1} w_{m_1,i} \sum_{j=1}^{m_2} w_{m_2,j}\, V_l(x_{m_1,i}, x_{m_2,j}) =: Q_{m_1,m_2} \tag{46}$$

where

$$V_l(r_1,r_2) = \frac{g(G_l(D((r_1+1)/2,(r_2+1)/2)))(r_1+1)/2}{|\alpha_i(s_1,s_2) - \alpha_i(G_l(D((r_1+1)/2,(r_2+1)/2)))|} \quad l = 1,\ldots,4 \quad -1 \leqslant r_1, r_2 \leqslant 1$$

Several numerical tests have shown that this procedure gives high accuracy already for low values of m_1 and m_2, when (s_1,s_2) is not too close to the sides of the square $[-1,1]\times[-1,1]$; when P approaches the boundary of the domain of integration then the accuracy deteriorates. For example, in Table XVII we have reported the relative errors obtained applying the above numerical procedure to the following integral:

$$\int_{-1}^{1}\int_{-1}^{1} \frac{\mathrm{d}\sigma_1\,\mathrm{d}\sigma_2}{\sqrt{(s_1-\sigma_1)^2 + (s_2-\sigma_2)^2}} \quad (s_1,s_2) \in [-1,1]\times[-1,1] \tag{47}$$

Note that this integral can be obtained in particular from the single layer potential $\int_{S_1} \mathrm{d}S_Q/|P-Q|$, over the face S_1 of the cube $\Omega = [-1,1]\times[-1,1]\times[-1,1]$ parametrized by

$$p_1 : (s_1,s_2) \in [-1,1]\times[-1,1] \to (1,s_1,s_2) \in S_1 \subset \Omega$$

and with $P \in S_1$.

In Table XVII we have chosen $m_1 = \bar{m}_1 = 2$, because in the final integral the integrand depends only on the second variable. From Table XVII the loss of accuracy when the collocation point is close to the boundary of $[-1,1]\times[-1,1]$ shows up clearly. Since we have chosen as co-ordinates of the collocation points the zeros of orthogonal polynomials which, as it is well-known, thicken near the endpoints ± 1, the above problem is of particular importance. Therefore, for the evaluation of the integral (45) with $P \equiv \alpha_i(s_1,s_2)$ internal and close to the boundary of Δ_i, we have proposed a new numerical procedure. It is based on a smoothing transformation and it gives more accurate approximations than those obtained with the Duffy transformation, when (s_1,s_2) is near to the boundary of the square (see Tables XVIII and XIX). Moreover, as we shall see, it works also for the nearly singular

Table XVIII. Relative errors $|S_{\bar{m}_1,\bar{m}_2} - S_{m_1,m_2}|/|S_{\bar{m}_1,\bar{m}_2}|$ for the integral (47) with $\bar{m}_1 = 128$, $\bar{m}_2 = 256$, $m_1 = m_2/2$.

	$s_1 = s_2 = 0.99$			$s_1 = s_2 = 0.999$			$s_1 = 0.999$ $s_2 = 0$		
m_2	$p = 3$	$p = 5$	$p = 7$	$p = 3$	$p = 5$	$p = 7$	$p = 3$	$p = 5$	$p = 7$
4	$5.52-02$	$1.20-01$	$1.40-01$	$4.85-02$	$1.33-01$	$2.82-02$	$2.29-01$	$1.02-02$	$3.07-01$
8	$1.07-02$	$5.35-03$	$1.43-02$	$3.36-03$	$2.90-02$	$1.82-02$	$2.90-02$	$1.76-02$	$2.90-02$
16	$2.15-03$	$6.33-04$	$4.03-04$	$2.42-04$	$2.15-04$	$3.80-04$	$4.63-03$	$3.07-04$	$5.34-04$
32	$2.12-04$	$9.63-06$	$6.51-06$	$4.84-05$	$2.12-06$	$9.30-06$	$1.17-03$	$9.10-05$	$2.56-05$
64	$2.42-05$	$4.96-07$	$3.31-08$	$1.06-05$	$1.25-07$	$6.71-08$	$1.63-04$	$2.94-07$	$4.05-07$
128	$2.61-06$	$6.05-09$	$1.85-10$	$9.91-07$	$3.00-09$	$1.26-10$	$1.76-05$	$3.65-08$	$1.20-09$

Table XIX. Relative errors $|S_{\bar{m}_1,\bar{m}_2} - S_{m_1,m_2}|/|S_{\bar{m}_1,\bar{m}_2}|$ for the integral (50) with $\bar{m}_1 = 128$, $\bar{m}_2 = 256$, $m_1 = m_2/2$.

	$s_1 = s_2 = 0.9$			$s_1 = s_2 = 0.99$			$s_1 = 0.99$ $s_2 = 0$		
m_2	$p = 1$	$p = 3$	$p = 5$	$p = 1$	$p = 3$	$p = 5$	$p = 1$	$p = 3$	$p = 5$
4	$1.13-02$	$1.97-03$	$1.54-01$	$5.95-02$	$8.05-02$	$2.00-01$	$1.82-01$	$2.59-01$	$9.56-02$
8	$1.72-02$	$9.73-04$	$1.60-02$	$1.62-02$	$6.21-03$	$3.51-03$	$9.55-02$	$3.69-02$	$3.36-02$
16	$8.89-04$	$2.26-05$	$3.31-04$	$1.77-04$	$7.12-04$	$1.95-04$	$4.71-02$	$8.75-04$	$1.01-03$
32	$2.26-05$	$5.49-07$	$1.60-06$	$7.09-04$	$2.76-06$	$2.62-06$	$2.12-02$	$1.37-04$	$5.13-06$
64	$1.47-08$	$2.23-10$	$7.39-12$	$6.27-05$	$5.00-08$	$1.17-08$	$8.12-03$	$3.72-06$	$3.20-07$
128	—	—	—	$5.60-07$	$6.09-13$	$6.82-13$	$2.10-03$	$2.16-09$	$7.61-11$

integrals. The smoothing transformation we propose was already considered in Reference [7]. It is

$$\tilde{\gamma}(t) = x_0 + b_{x_0}(t - a_{x_0})^p \quad t \in [-1, 1] \quad p > 1 \tag{48}$$

where $x_0 \in [-1, 1]$ is given and p is a freely chosen odd positive integer, while a_{x_0} and b_{x_0} are determined by requiring $\tilde{\gamma}(-1) = -1$ and $\tilde{\gamma}(1) = 1$:

$$a_{x_0} = \frac{(1+x_0)^{1/p} - (1-x_0)^{1/p}}{(1+x_0)^{1/p} + (1-x_0)^{1/p}} \quad b_{x_0} = \frac{1 - x_0}{(1 - a_{x_0})^p}$$

Note that the leading derivatives of $\tilde{\gamma}$ all vanish at $a_{x_0} := \tilde{\gamma}^{-1}(x_0)$. After introducing in (44) with $k = i$, $\sigma_1 = s_1 + a_{s_1}(r_1 - b_{s_1})^p$ and $\sigma_2 = s_2 + a_{s_2}(r_2 - b_{s_2})^p$, we approximate the resulting integral by means of a standard product of Gauss–Legendre quadrature rules

$$I \approx \sum_{i=1}^{m_1} w_{m_1,i} \sum_{j=1}^{m_2} w_{m_2,j} U(x_{m_1,i}, x_{m_2,j}) =: S_{m_1,m_2} \tag{49}$$

where

$$U(r_1, r_2) = p^2 \frac{g(s_1 + a_{s_1}(r_1 - b_{s_1})^p, s_2 + a_{s_2}(r_2 - b_{s_2})^p)(r_1 - b_{s_1})^{p-1}(r_2 - b_{s_2})^{p-1}}{|\alpha_i(s_1, s_2) - \alpha_i(s_1 + a_{s_1}(r_1 - b_{s_1})^p, s_2 + a_{s_2}(r_2 - b_{s_2})^p)|}$$

In Table XVIII we have reported the relative errors obtained applying the smoothing procedure to approximate the integral (47).

By a comparison of Tables XVII and XVIII, we deduce that S_{m_1,m_2} is more efficient than Q_{m_1,m_2}; this because the complex poles, which affect Q_{m_1,m_2}, are moved away from the domain of integration by means of the smoothing change of variable. In addition, the computational cost of S_{m_1,m_2} is lower than that of Q_{m_1,m_2}; indeed, in the most general case, the number of function evaluations required by Q_{m_1,m_2} is $4m_1m_2$ if the domain of integration is a quadrangle ($3m_1m_2$ for triangular domains), while S_{m_1,m_2} requires only m_1m_2 function evaluations. In contrast, by comparing S_{m_1,m_2} with Q_{m_1,m_2} when (s_1,s_2) is internal to the domain of integration and far from the boundary of $[-1,1]\times[-1,1]$, we find that Q_{m_1,m_2} performs better than S_{m_1,m_2}. This is obvious because while the Duffy transformation removes the singularity, the smoothing change of variable only smoothes it. Therefore, we suggest to use the Duffy transformation when $(s_1,s_2)\in(-0.99,0.99)\times(0.99,0.99)$ and the smoothing transformation otherwise. As Table XIX shows, the smoothing change of variable (48) has revealed its efficiency also for the nearly singular integrals. As a numerical test we have considered the following integral:

$$\int_{-1}^{1}\int_{-1}^{1}\frac{\mathrm{d}\sigma_1\,\mathrm{d}\sigma_2}{\sqrt{(1+\sigma_1)^2+(s_1-1)^2+(s_2-\sigma_2)^2}}\quad (s_1,s_2)\in[-1,1]\times[-1,1] \tag{50}$$

which can be obtained from the single layer potential $\int_{S_2}\mathrm{d}S_Q/|P-Q|$, over the face S_2 of the cube $S=[-1,1]\times[-1,1]\times[-1,1]$ parametrized by

$$p_2:(s_1,s_2)\in[-1,1]\times[-1,1]\to(-s_1,1,s_2)\in S_2\subset S$$

and with $P\in S_1$, where S_1 is the face of S above considered. In this case we have introduced in (50) $\sigma_1=-1+a_{-1}(r_1-b_{-1})^p$ and $\sigma_2=s_2+a_{s_2}(r_2-b_{s_2})^p$ and, then, applied a product of Gauss–Legendre quadrature rules. By comparing the numerical results obtained when $p=1$ and when $p>1$ we remark that in the case of nearly singular integrals the smoothing approach is efficient already for $(s_1,s_2)\in[-1,1]\times[-1,1]\backslash[-0.9,0.9]\times[-0.9,0.9]$.

The last numerical test we consider, to show the efficiency of the smoothing procedure, is a single layer integral over a xy-planar triangle Δ, whose vertices are $(0,0)$, $(-1/4,1/4)$, $(-1/4,-1/4)$:

$$\int_{\Delta}\frac{\mathrm{d}\Delta_Q}{|P-Q|}=\int_{-1/4}^{0}\int_{-x}^{x}\frac{\mathrm{d}y\,\mathrm{d}x}{\sqrt{(x-a_1)^2+(y-a_2)^2+a_3^2}} \tag{51}$$

being $Q\equiv(a_1,a_2,a_3)\in\Re^3$. We have chosen Q first inside and then outside Δ and used the smoothing procedure described above. The relative errors obtained by using the quadrature formula S_{m_1,m_2} and fixing Q equal to $(-0.01,-0.005,0)$, $(-0.01,0,0.005)$ and $(0.01,0,0)$ are reported in Table XX.

Test 7

In this last numerical test we solve a problem of type (34) with $\Omega=[-1,1]\times[-1,1]\times[-1,1]$ by applying to the BIE (36) the collocation method proposed in Section 5. In this particular example, we have assumed $u=x^2-z^2$ on Ω and we have set $u:=\bar{f}$ on the boundary $S=\partial\Omega$. Moreover, we have decomposed S in its six planar faces S_i and ψ_i, $i=1,\ldots,6$,

Table XX. Relative errors $|S_{\bar{m}_1,\bar{m}_2} - S_{m_1,m_2}|/|S_{\bar{m}_1,\bar{m}_2}|$ for the integral (51) with $\bar{m}_1 = \bar{m}_2 = 256$, $m_1 = m_2$.

	$Q = (-0.01, -0.005, 0)$			$Q = (-0.01, 0, 0.05)$		$Q = (0.01, 0, 0)$	
m_2	$p = 1$	$p = 3$	$p = 5$	$p = 1$	$p = 3$	$p = 1$	$p = 3$
4	2.18 − 02	1.47 − 02	2.89 − 02	4.91 − 02	7.57 − 03	7.70 − 03	1.35 − 03
8	8.49 − 02	2.04 − 03	1.59 − 03	1.45 − 02	9.59 − 04	3.89 − 04	1.47 − 09
16	4.56 − 02	2.25 − 04	6.82 − 05	1.56 − 02	3.58 − 05	1.31 − 07	2.45 − 12
32	2.40 − 02	1.05 − 04	2.24 − 06	2.90 − 05	1.48 − 07	1.12 − 10	—
64	1.29 − 02	1.44 − 05	8.16 − 08	6.74 − 09	—	—	—
128	4.65 − 03	1.19 − 06	1.88 − 09	—	—	—	—

Table XXI. Relative errors in Test 7.

	$\|u(P) - u_n(P)\|/\|u(P)\|$ at $P = (0.1, 0.15, 0.15)$		$\|u(P) - u_n(P)\|/\|u(P)\|$ at $P = (0.6, 0.5, 0.5)$	
n	$q = 1$	$q = 2$	$q = 1$	$q = 2$
2	6.27 − 02	4.60 − 01	8.53 − 02	4.15 − 01
4	5.37 − 03	2.83 − 02	1.20 − 02	2.04 − 02
6	4.28 − 04	2.26 − 04	3.64 − 04	7.87 − 04
8	1.31 − 04	3.95 − 05	8.69 − 05	2.04 − 04
10	6.48 − 06	2.86 − 05	1.32 − 04	1.28 − 04
12	1.43 − 05	1.80 − 06	4.85 − 06	1.29 − 06

are sought on S_i. Therefore, after having introduced a parametrization p_i of the faces S_i, defined on the square $[-1,1]\times[-1,1]$, we have smoothed the unknowns along the boundary of this square. The system we have then solved is given by (43), where $\bar{l} = 6$ and $\alpha_i = p_i(\gamma)$, $i = 1,\ldots,6$, with γ given by (7). The matrix elements (44) have been evaluated in a suitable way. More precisely, when the collocation point $P = \alpha_k(s_1, s_2)$ belongs to the integration domain, i.e. $k = i$, and $q = 1$, then we have approximated the corresponding integrals by means of the following quadrature rules: Q_{m_1,m_2} with $m_1 = m_2 = n$ if $(s_1, s_2) \in [-0.5, 0.5]\times[-0.5, 0.5]$, Q_{m_1,m_2} with $m_1 = m_2 = 2n$ if $(s_1, s_2) \in [-0.99, 0.99]\times[-0.99, 0.99]\backslash[-0.5, 0.5]\times[-0.5, 0.5]$, S_{m_1,m_2} with $p = 5$ and $m_1 = m_2 = 2n$ if $(s_1, s_2) \in [-1,1]\times[-1,1]\backslash[-0.99, 0.99]\times[-0.99, 0.99]$. Moreover, this latter formula has been used also when the collocation point is outside but close to the domain of integration. In particular, when $(s_1, s_2) \in [-1,1]\times[-1,1]\backslash[-0.9, 0.9]\times[-0.9, 0.9]$ and P belongs to a face which is adjacent to the integration face. As already remarked in Section 2.1, the smoothing transformation produces a concentration of points with exponent q in the neighbourhood of the boundary. Therefore, when $q = 2$ we have considered in the situations above $[-0.9, 0.9]\times[-0.9, 0.9]$ instead of $[-0.99, 0.99]\times[-0.99, 0.99]$, and $[-0.68, 0.68]\times[-0.68, 0.68]$ instead of $[-0.9, 0.9]\times[-0.9, 0.9]$.

In Table XXI we have reported the relative errors in the computation of $u(0.1, 0.15, 0.15)$ and $u(0.6, 0.5, 0.5)$.

As one can see in Table XXI, for relative errors up to 10^{-5} there is not much difference between the cases $q = 1$ and 2. Probably, the case $q = 2$ shows its higher accuracy when n

assumes larger values than 12. This is due, as we have already remarked, to the flatness of the smoothing transformation near the edges.

The collocation method presented in this section requires to transform boundary triangle elements into squares. This to construct simple smoothing transformations and two dimensional polynomial approximations. Of course, it would be more efficient to work directly on triangles, that is to consider smoothing transformations and polynomials (of total degree n) defined on a reference triangle. This will be a subject of a future investigation.

ACKNOWLEDGEMENTS

This work was supported by the Ministero dell'Università e della Ricerca Scientifica e Tecnologica of Italy and by the Consiglio Nazionale delle Ricerche under contract No. 98.00648.CT11.

REFERENCES

1. Atkinson KE. *The Numerical Solution of Integral Equations of the Second Kind.* Cambridge University Press: Cambridge, 1997.
2. Elschner J, Graham IG. An optimal order collocation method for first kind boundary integral equations on polygons. *Numerische Mathematik* 1995; **70**:1–31.
3. Elschner J, Jeon Y, Sloan IH, Stephan EP. The collocation method for mixed boundary value problem on domains with curved polygonal boundaries. *Numerische Mathematik* 1997; **76**:355–381.
4. Kress R. A Nyström method for boundary integral equations in domains with corners. *Numerische Mathematik* 1990; **58**:145–161.
5. Monegato G, Scuderi L. High order methods for weakly singular integral equations with nonsmooth input functions. *Mathematics of Computation* 1998; **67**:1493–1515.
6. Monegato G, Scuderi L. Global polynomial approximation for Symm's equation on polygons. *Numerische Mathematik* 2000; **86**:655–683.
7. Monegato G, Sloan IH. Numerical solution of the generalized airfoil equation for an airfoil with a flap. *SIAM Journal on Numerical Analysis* 1997; **34**:2288–2305.
8. Prössdorf S, Rathsfeld A. Quadrature methods for strongly elliptic Cauchy singular integral equations on an interval. In *The Gohberg Anniversary Collection, Topics in Analysis and Operator Theory*, Dym H *et al.* (eds), vol. 2. Birkhäuser Verlag: Basel, 1989; 435–471.
9. Scuderi L. A collocation method for the generalized airfoil equation for an airfoil with a flap. *SIAM Journal on Numerical Analysis* 1998; **35**:1725–1739.
10. Scuderi L. A Chebyshev polynomial collocation BIEM for mixed boundary value problems on nonsmooth boundaries. *Journal of Integral Equations and Applications* 2002; **14**:179–221.
11. Yan Y, Cosine change of variable for Symm's integral equation on open arcs. *IMA Journal of Numerical Analysis* 1990; **10**:521–535.
12. Yan Y, Sloan IH. On integral equations of the first kind with logarithmic kernels. *Journal of Integral Equations and Applications* 1988; **1**:549–579.
13. Evans G. *Practical Numerical Integration.* Wiley: New York, 1993.
14. Monegato G, Scuderi L. Numerical integration of functions with boundary singularities. *Journal of Computational and Applied Mathematics* 1999; **112**:201–214 [Special Issue: Numerical Evaluation of Integrals, Laurie D, Cools R (eds).]

